A Kinetic Model for the Deterministic Prediction of Gel-Based Single-Chirality Single-Walled Carbon Nanotube Separation

Kevin Tvrdy,[†,§] Rishabh M. Jain,[‡,§] Rebecca Han,[†] Andrew J. Hilmer,[†] Thomas P. McNicholas,[†] and Michael S. Strano[†,*]

[†]Departments of Chemical Engineering and [‡]Materials Science Engineering, Massachusetts Institute of Technology, 77 Massachusetts Avenue, Cambridge, Massachusetts 02139, United States. [§]These authors contributed equally to this work.

ABSTRACT We propose a kinetic model that describes the separation of single-chirality semiconducting carbon nanotubes based on the chirality-selective adsorption to specific hydrogels. Experimental elution profiles of the (7,3), (6,4), (6,5), (8,3), (8,6), (7,5), and (7,6) species are well described by an irreversible, first-order site association kinetic model with a single rate constant describing the adsorption of each SWNT to the immobile gel phase. Specifically, we find first-order binding rate constants for seven experimentally separated nanotubes normalized by the binding site molarity (M_θ): $k_{7,3} = 3.5 \times 10^{-5}\ M_\theta^{-1}\ s^{-1}$, $k_{6,4} = 7.7 \times 10^{-8}\ M_\theta^{-1}\ s^{-1}$, $k_{8,3} = 2.3 \times 10^{-9}\ M_\theta^{-1}\ s^{-1}$, $k_{6,5} = 3.8 \times 10^{-9}\ M_\theta^{-1}\ s^{-1}$, $k_{7,5} = 1.9 \times 10^{-11}\ M_\theta^{-1}\ s^{-1}$, $k_{8,6} = 7.7 \times 10^{-12}\ M_\theta^{-1}\ s^{-1}$, and $k_{7,6} = 3.8 \times 10^{-12}\ M_\theta^{-1}\ s^{-1}$. These results, as well as additional control experiments, unambiguously identify the separation process as a selective adsorption. Unlike certain chromatographic processes with retention time dependence, this separation procedure can be scaled to arbitrarily large volumes, as we demonstrate. This study provides a foundation for both the mechanistic understanding of gel-based SWNT separation as well as the potential industrial-scale realization of single-chirality production of carbon nanotubes.

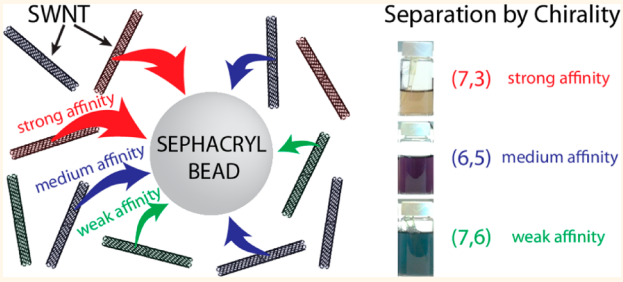

KEYWORDS: single-walled carbon nanotube · single chirality · separation · sodium dodecyl sulfate · sephacryl gel

Single-walled carbon nanotubes (SWNTs) have promising applications that include biological sensing[1,2] and optoelectronics.[3−6] However, because SWNTs demonstrate electronic properties (metallic *vs* semiconducting of various band gap) based on slight variations in their chiral wrapping vector (*n*,*m*),[7] their inclusion in laboratory-scale devices has largely been limited to applications where electronic heterogeneity is tolerable. In order to better understand the chirality-dependent properties of SWNTs and to further utilize those properties in practical devices, it is necessary to separate preparative-scale quantities of SWNTs according to specific SWNT chirality. Initial work by Kappes and co-workers demonstrated the ability of an amide-functionalized hydrogel (Sephacryl S200) to separate metallic and semiconducting SWNTs suspended in sodium dodecyl sulfate (SDS).[8] Further progress was made by Kataura and co-workers, who used multiple iterations of a single-surfactant process to yield 13 unique semiconducting SWNT types, ranging in purity from 46 to 94%.[9] Here, we further develop the understanding of hydrogel-based single-chirality SWNT separation by modeling the interactions of individual chiralities of semiconducting SWNTs with amide-functionalized hydrogels. We classify this process as a kinetically driven selective adsorption reaction and, through modeling experimental results as such, estimate chirality-dependent rate constants for the interaction of semiconducting SWNTs with separation gel media. A more thorough understanding of single-chirality SWNT separation has implications for process scalability, which we achieve here at 15 times larger volume than what has been previously demonstrated experimentally.

* Address correspondence to strano@mit.edu.

Received for review December 21, 2012 and accepted January 25, 2013.

Published online January 25, 2013
10.1021/nn305939k

The separation of SWNTs by chirality has been an important research focus since their discovery. Bottom-up approaches toward separation attempt to control ensemble scale growth through the use of specialized catalytic nanoparticles and SWNT growth conditions.[10,11] For example, SWeNT's SG65i growth process results in a 40% enrichment of the (6,5) chirality.[12] On the other hand, top-down approaches toward separation, which attempt to isolate specific electronic types or chiralities using post-growth processing, have seen success using electrophoretic,[13−20] selective chemical reactivity,[21−23] density gradient ultracentrifugation (DGU),[24−29] and gel-based retention methods.[9,30]

Separation by DGU, which utilizes ultracentrifugation of SWNT suspensions in the presence of a density gradient to isolate single SWNT chiralities by relative buoyant density, has proven commercially viable[31] yet relies on a centrifugation step that is not scalable, inherently limiting mass production of single-chirality materials. SWNT separation based on selective gel retention, on the other hand, has the potential for less expensive processing while producing relatively pure single-chirality semiconducting samples. Kataura and co-workers demonstrated for the first time a large-scale gel-based separation that produces near-single-chirality samples from a mixture of nanotubes produced using the HiPco process.[9] Our group slightly modified this process to generate large quantities of pure (6,5) SWNTs in a single pass of HiPco SWNT through sephacryl, enabling the creation of the first single-chirality all-carbon solar cell.[32]

The mechanism for separation using either DGU or gel retention methods remains speculative due to the complicated nature of experimentally determining molecular dynamics at the nanoscale. For example, models suggest that the chirality-dependent buoyant density that allows for chiral selectivity *via* DGU may be caused by chiral-specific packing of surfactant molecules on the surface of semiconducting SWNTs.[33] Ziegler and co-workers described the mechanistic interaction of SWNTs with agarose gel as a chromatography governed by the morphology of SDS on the surface of a SWNT.[34] Further, Kataura and co-workers have described the adsorption of SDS-suspended SWNTs with either agarose or sephacryl as a batch adsorption process, specifically determining energetic changes in the adsorption of semiconducting *versus* metallic SWNTs to each separation medium.[35]

In this article, we quantitatively and mechanistically describe the process by which single-chirality carbon nanotubes are separated from a sample of HiPco nanotubes using hydrogels. We demonstrate that the separation of single-chirality SWNTs is a kinetically driven forward adsorption process, using the same gel medium utilized by Kataura and co-workers in their initial work.[9] The agreement between our experimentally observed and model-predicted separations, and the assignment of chirality-specific rate constants describing the binding of semiconducting SWNTs to sephacryl gel, provides a basis for the future understanding and modification of the laboratory and industrial-scale separation of semiconducting SWNTs using functionalized hydrogels.

RESULTS AND DISCUSSION

The SWNT separation procedure utilized here is a modified version of the methodology previously published by Kataura and co-workers.[9] Specifically 10 mL of a 1 mg/mL SWNT suspension in 70 mM aqueous SDS (see Methods section and Supporting Information Figure S1 for SWNT solution preparation and characterization, respectively) is passed through a 1.4 mL stationary bed of 70 mM SDS equilibrated Sephacryl S200 gel at 1 mL/min. Following interaction with the sephacryl gel, passed SWNT solution was collected and set aside for repeated gel-pass iterations (Figure 1, step 1). By using this technique, total per column residence time was held constant, a step that was not taken in previous descriptions of stacked, cascade style column-to-column flow.[9] We believe that controlling this aspect of the separation aids in the overall repeatability of the procedure as well as contributes to the purity of the separated single-chirality SWNT, as discussed later. The gel is then washed with 4 mL of 70 mM SDS solution to remove any SWNTs that are not adsorbed to the medium (Figure 1, step 2). Finally, adsorbed SWNTs are eluted from the gel through the passing and collection of 4 mL of 175 mM SDS solution (Figure 1, step 3).

Repeated iterations of this process are performed, whereby the flow through from step 1 is utilized as the starting material for step 1 in the proceeding iteration. The elapsed time between iterations is minimized to ∼15 min per iteration. Material eluted by 175 mM SDS is labeled as "column 1" for the first procedural iteration, and subsequent iterations are labeled in numerical order. A diagram for the complete process is shown in Figure 1, and further details of the method are presented in the Methods section.

As SWNTs are passed through a stationary sephacryl gel bed, those with the largest affinity for the gel are selectively removed from the bulk solution during early separation iterations (early columns), while those with relatively less affinity are selectively removed at later iterations. This process has been utilized to yield few-chirality samples by Kataura and co-workers, whereas multiple separation stages (running the separated material from a primary stage through a secondary set of columns) were necessary to achieve near single-chirality separation.[9] A full list of separable species through multistage gel separation, along with their separation order, has been published elsewhere.[9]

We carried out a typical separation as described in the Methods section such that bulk SWNT solution was

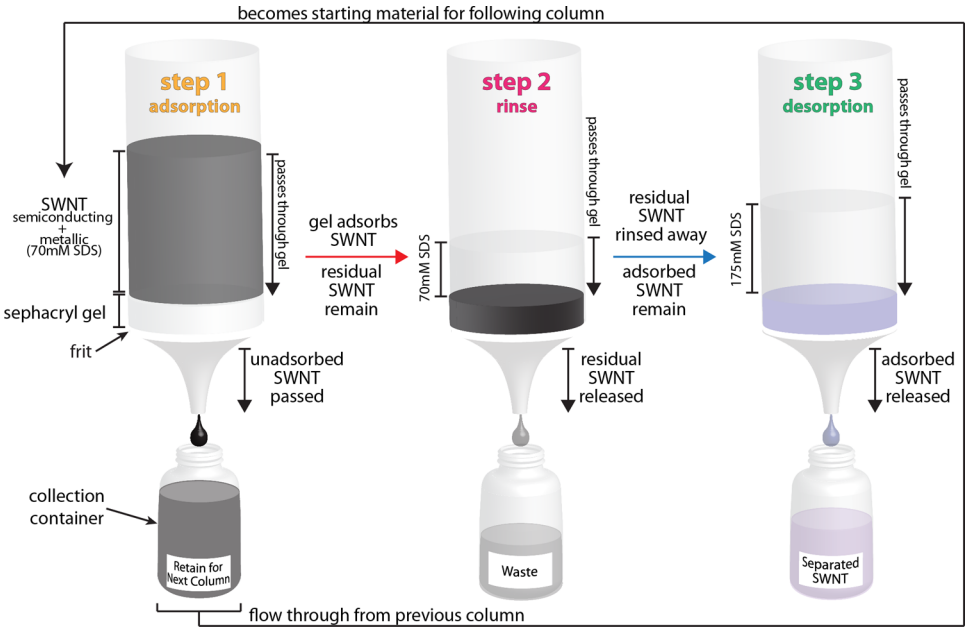

Figure 1. Illustration of the three-step process utilized to perform a single adsorption column of single-chirality semiconducting SWNT separation. Step 1: passing of a SWNT mixture through a sephacryl gel bed, resulting in selective adsorption of SWNT to gel. Step 2: rinsing of residual, non-adsorbed SWNT from the gel using SWNT-free 70 mM SDS solution. Step 3: desorption of bound SWNT from gel through passing of SWNT-free 175 mM SDS solution through gel/SWNT matrix. Note that this process is explicitly different from previously published sephacryl-gel-based SWNT separations as we do not form a cascade of columns but rather pool together material following step 1 from each column and use it as the staring material for the subsequent column.

iteratively flowed through repeated columns of fresh sephacryl until no significant adsorption of SWNTs onto or desorption of SWNTs from a sephacryl bed column was noted. The resultant per column absorption spectra of the solution eluted during the 175 mM desorption step over the course of a 20 column separation are illustrated in Figure 2 (see Figure S2 for a Y offset waterfall plot). Note that, while slight variance does exist when experimental conditions are repeated, the separation represented in Figure 2 represents a typical separation carried out under described conditions and will be the basis for the predicted model later developed in this work.

Figure 2 illustrates the general trend of increasing diameter with column number, similar to that observed by Kataura.[9] It is also interesting to note that by the 20th column the absolute absorbance value reduces, indicating that the amount of SWNT being absorbed to the column is generally reduced with increasing columns number.

In order to quantitatively describe the chirality distribution obtained from each elution, we fit the nanotube absorbance profiles to Lorentzian curves in the lowest energy excitation peak (E_{11}, 800 nm −1300 nm) region after subtracting a linear background. Within the 20 column separation, we were able to spectroscopically identify the separation of seven unique semiconducting SWNT species. The best fit peak summation for eluted samples that contain both single and multiple SWNT chiralities is shown in Figure 3A, along with fit residuals. Further details of the fitting technique is described in the Supporting Information (Figure S3). The best fit relative absorbance of each

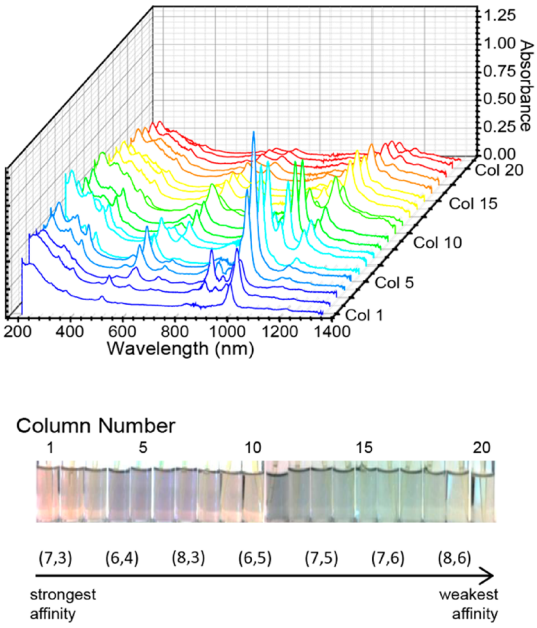

Figure 2. Absorption spectra of semiconducting SWNTs desorbed from sephacryl over the entirety of a 20 column separation run with 10 mL of SWNT solution through 1.4 mL of Sephacryl S200 at a 1 mL/min adsorption where fresh sephacryl was used for each iterative column. Detailed experimental conditions are detailed in the Methods section. A photograph of a 20 column separation is also shown, displaying coloration of the nanotube solutions from yellow, to purple, to blue, to green. Note that the coloration becomes weak at the end as the concentration of SWNTs decreases at the end of the separation.

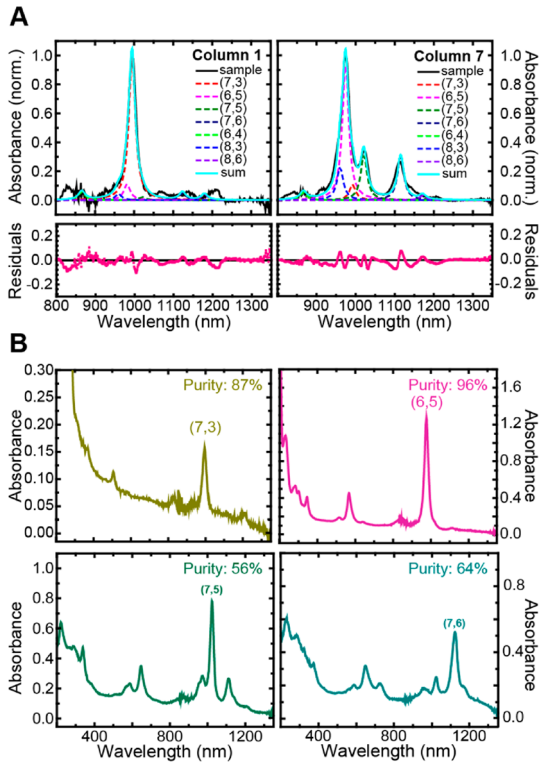

Figure 3. (A) Absorption spectra (solid black line) and best fit Lorentizan profiles (dashed lines) of extracted semiconducting nanotube solutions from both a single-chirality column (column 1) as well as a mixed-chirality column (column 7). Both of these samples are taken from the 20 column separation shown in Figure 2. (B) Absorption spectra of specific single columns highlighting the ability of this process to generate chirally pure and highly enriched semiconducting SWNT samples. Note that purities reported were calculated using the peak fitting algorithm described in the Supporting Information.

chirality present in a given elution was then used to estimate the effective purity of that solution.

Further, given the previously calculated chirality-dependent length density of carbon atoms in semiconducting SWNTs,[7] the previously reported per carbon atom optical cross section for (6,5) semiconducting SWNTs[36] of $\sigma = 1.7 \times 10^{-17}$ cm^2 (and assuming this value is constant across all chiralities), and using the average separated length of semiconducting SWNT obtained from this procedure[32] $\langle l \rangle = 300$ nm, it is possible to assign a chirally dependent absolute number of extracted SWNTs per column. Although it remains purely an estimate of the per column number of separated SWNTs, this parameter is necessary when formulating a SWNT separation model that accounts for a 1:1 binding ratio between semiconducting SWNTs and sephacryl binding sites, as we do in the second part of this work.

In contrast to previous reports, here we demonstrate the generation of chirally pure and highly enriched SWNT samples utilizing only a single pass of the starting SWNT material through a series of sephacryl gel columns. Specifically, we report the (6,5) chirality as 96% pure, which is more pure than previously reported separations using either DGU or gel separation. Further, we report the (7,3), (7,5), and (7,6) highly enriched samples as 87, 56, and 64% pure, respectively, each significantly more pure than what was realized previously during a first-pass separation.[9] The absorbance spectrum of each of these single-chirality and highly enriched samples is shown in Figure 3B.

To further investigate the effects of SWNT/sephacryl interaction on the separation quality, we designed an alternative scheme whereby instead of 10 mL of SWNT solution flowing through a stationary 1.4 mL sephacryl bed, 10 mL of SWNT solution and 1.4 mL of sephacryl were vigorously mixed together inside a round-bottom flask for 10 min, the same amount of time required to complete a single flowed-through column. Following mixing with SWNT solution, sephacryl was then physically isolated by pouring the SWNT/sephacryl mixture into an empty fritted column and applying an overpressure to pass the SWNT solution through the column in ~15 s, whereas the sephacryl and selectively adsorbed SWNT were retained by the frit. The sephacryl was then processed in an identical manner as the flow-through scheme following SWNT adsorption (Figure 1, steps 2−3).

Processing the same starting material side-by-side in both a flowed-through and stirred manner provided insight into the nature of sephacryl-gel-based SWNT separation and direction toward the construction of a model to describe it. Interestingly, a side-by-side comparison of the per column absorbance features of the separation carried out in these two fundamentally unique procedures yielded nearly identical results. Specifically, separation order, quantity of chirality-specific SWNT separated, and number of columns required to separate the same amount of material were qualitatively the same through 10 iterative columns of SWNT separation (Figure S4). In terms of designing a gel-based SWNT separation model, this finding suggests that regardless of the physical nature of the SWNT/sephacryl interaction (flowed or stirred) the resultant separation behaves as though the two are well-mixed. The following section describes in detail the formulation of a SWNT separation model that predicts the experimental observations made here.

Kinetically Driven Competitive Binding Model. *Binding Model Formulation.* Given the observed equivalency between a separation carried out such that (1) SWNTs flow through a stationary bed of sephacryl gel held by a porous frit, and (2) SWNTs and sephacryl gel were physically mixed and later separated using a porous frit; we developed a model that describes the gel-assisted separation of SWNTs based on the principles of a series of well-mixed semibatch reactors, such that each subsequent adsorption "reactor" models a single column of SWNT separation. This model is grounded in the assumption that within each column there exists a total

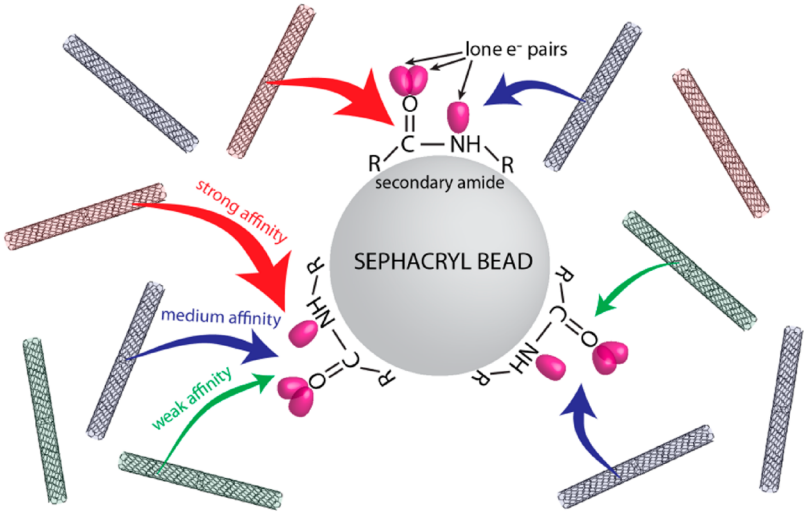

Figure 4. Cartoon depiction of the kinetically driven competitive binding model we developed to describe the single-chirality separation of semiconducting SWNTs. Carbon nanotube chiralities with the strongest affinity for secondary amide groups present on the surface of sephacryl hydropolymer beads bind first to those sites, allowing for their selective extraction as a chirally pure aliquot.

total number of generic sephacryl binding sites, θ_T, each of which may bind to any chirality of semiconducting SWNT. Further, semiconducting SWNTs interact with empty sephacryl binding sites at a given time, $\theta(t)$, in a chiral-specific manner, such that SWNTs of like chirality have like binding affinities for unoccupied sephacryl sites (Figure 4). Here, we suggest that a sephacryl binding site for a semiconducting SWNTs is enabled by secondary amide groups displayed along the polymer backbone, as proposed by others.[37,38]

The binding of semiconducting SWNTs to an unoccupied sephacryl site is generally described by the interaction of each SWNT chirality, $N_{n,m}$, with an empty sephacryl binding site, θ, such that following a binding event, a bound SWNT$_{n,m}$/sephacryl pair, $P_{n,m}$, is created:

$$N_{n,m} + \theta \underset{k^r_{n,m}}{\overset{k^f_{n,m}}{\rightleftharpoons}} P_{n,m} \quad (1)$$

where $k^f_{n,m}$ and $k^r_{n,m}$ are the forward and reverse rate constants, respectively, of the chirality-dependent interaction between a SWNT and an unoccupied binding site. Here, the subscripts (n,m) designate the wrapping vectors n and m which are commonly used to assign SWNTs by chirality.[7] The chirality-dependent equilibrium constant, $K_{n,m}$, can then be written in terms of the forward and reverse rate constants.

$$K_{n,m} = \frac{k^f_{n,m}}{k^r_{n,m}} \quad (2)$$

Within each sephacryl column, there exists a finite amount of sephacryl and thus a finite number of binding sites. To maintain a balance of available binding sites, it is necessary to hold the total number of unoccupied sites, θ, along with the sum of total number of bound SWNT$_{n,m}$/sephacryl pairs, $P_{n,m}$, constant and equivalent to the total number of available binding sites per column, θ_T

$$\theta(t) + \sum_{n,m} P_{n,m}(t) = \theta_T \quad (3)$$

where, here, the time dependence of both $\theta(t)$ and $P_{n,m}(t)$ is explicitly written, as binding events are dynamic over the course of SWNT/sephacryl interaction. We can then write the time-dependent change in number of free SWNTs, $N_{n,m}$, within a well mixed reaction volume V as

$$-\frac{d(N_{n,m})}{dt} = \frac{k^f_{n,m}}{V}(N_{n,m})(\theta) - \frac{k^f_{n,m}}{VK_{n,m}}(P_{n,m}) \quad (4)$$

The adsorption is assumed to be isochoric. Substituting site balance terms into eq 4 for θ and $P_{n,m}$ yields

$$-\frac{d(N_{n,m})}{dt} = \frac{k^f_{n,m}}{V}(N_{n,m}(t))\left(\theta_T - \sum_{n,m}(N_{n,m}(t_0) - N_{n,m}(t))\right) - \frac{k^f_{n,m}}{VK_{n,m}}(N_{n,m}(t_0) - N_{n,m}(t)) \quad (5)$$

Here, it is important to note that experimental attempts were made to demonstrate the reversibility of reaction 1 but were not fruitful. Specifically, following the sephacryl rinsing step (Figure 1, step 2), which was carried out at 70 mM SDS concentration, we made attempts to release the adsorbed SWNTs from the sephacryl by passing copious amounts of 70 mM SDS solution through the sephacryl and monitoring the absorbance of the passed solution, which showed no traces of desorbed SWNTs. If this reaction remained at equilibrium at 70 mM SDS, the addition of neat surfactant solution would shift the equilibrium to the reactant side and result in the desorption of bound SWNTs. We conclude, then, that SWNTs adsorbed to sephacryl at 70 mM SDS concentration do so irreversibly and thus

TABLE 1. Experimentally Determined Values for Initial Number of Chirality-Specific Semiconducting SWNTs Present in Starting Suspension ($N_{n,m}$), along with Best Fit Values for Initial Number of Carbon Impurities and Binding Rate Constants Describing the Chirality-Specific Interaction of SWNTs with Sephacryl

	carbon impurities	(7,3)	(6,4)	(8,3)	(6,5)	(7,5)	(8,6)	(7,6)
$N_{n,m}$ (col = 1, t = 0)	6.3×10^{14}	9.2×10^{13}	5.7×10^{13}	7.9×10^{13}	5.9×10^{14}	2.8×10^{14}	4.0×10^{13}	6.8×10^{14}
$k_{n,m}$ (M_θ^{-1} s^{-1})	3.8×10^{-6}	3.5×10^{-5}	7.7×10^{-8}	2.3×10^{-9}	3.8×10^{-9}	1.9×10^{-11}	7.7×10^{-12}	3.8×10^{-12}

construct this model not under equilibrium but rather as a series of forward binding rate constants. The removal of a desorption reaction at 70 mM SDS is realized through the elimination of the last term in eq 5.

Finally, we describe the second-order kinetics in terms of reactant and product concentrations, where we write the rate constant k^f in units of M_θ^{-1} s^{-1}, where M_θ is the concentration of binding sites on the sephacryl. We can explicitly write the volume of the sephacryl and that of the SWNT separately, where the concentration of binding sites on the sephacryl is a constant:

$$-\frac{d(M_{n,m})}{dt} = k^f_{n,m}(M_{n,m}(t))\left(\frac{\theta_T}{V_{seph}} - \sum_{n,m}(M_{n,m}(t_0) - M_{n,m}(t))\right) \quad (6)$$

where $M_{n,m}$ is the chirality-dependent molar concentration of SWNTs and V_{seph} is the volume of the sephacryl. Note that the only time-dependent term of eq 6 is the chirality-dependent concentration of unbound SWNTs, and thus this equation represents the most simplified expression for describing the dynamic binding of SWNTs to sephacryl. Equation 6 consists of a series of interdependent differential equations, each of which represents the time-dependent change of a specific chirality of SWNTs in the presence of a finite number of sephacryl binding sites. Because of this, it is necessary to solve this series of nonlinear differential equations numerically. A detailed description of the numerical procedure specifically used to solve for the time-dependent binding of SWNTs to sephacryl in each column is provided in the Supporting Information.

Modeling SWNT Solution and Sephacryl Gel. To compare simulated data with experimentally conducted separations, as we do here for the separation shown in Figure 2, initial values for $N_{n,m}$ were calculated by summing the amount of each chirality experimentally extracted over the entirety of the 20 column separation. The result of this summation was a mixture of seven semiconducting SWNT species of varying quantity. After 20 passes through fresh gel, the eluted SWNT solution still contained trace quantities of the (7,6) chirality, suggesting that this chirality was not entirely depleted from the bulk solution; therefore, the total amount collected over the course of 20 elutions is less than the total amount of (7,6) SWNT initially present in solution. To compensate for this discrepancy, 1.5 times the separated amount of (7,6) was substituted for $N_{7,6}$ in the simulated bulk SWNT solution.

Note that this estimate is only an approximation of the original solution, which also contains metallic SWNTs as well as other semiconducting species. However, it is well-documented that metallic SWNTs do not interact with hydrogels commonly used for SWNT separation[9,39] and thus can be excluded here. Further, while SDS suspensions of HiPco SWNTs are known to contain greater than seven semiconducting chiralities,[40] here such were either not separated by this procedure or were separated in such small quantities that identification *via* absorbance spectroscopy was not straightforward. Regardless, the limitation of this analysis to seven semiconducting species provides ample experimental data from which the quality of the model can be judged. The total number of SWNTs for each modeled chirality before it interacts with the first column of sephacryl ($N_{n,m}$ (col = 1, t = 0)) is listed in Table 1.

Further, it was observed that, upon elution of the columns, especially the initial columns, the gel retained a dark coloration even after the elution (Figure 5C). Hence, there is material retained on the column that does not elute with the 175 mM SDS solution. In order to investigate the nature of this material, a column that was eluted with 175 mM SDS was then eluted with sodium cholate (SC). Upon elution with 46 mM sodium cholate, the column was still colored; however, some of the previously adsorbed material was released, and while the absorbance spectrum (Figure 5B) of this elution shows evidence of some amount of SWNT, it primarily indicates the presence of carbon impurities such as fullerenes, small nanotube fragments, and bundles that typically comprise the background of SWNT solutions.[41]

Examination of the experimentally extracted SWNT species over 20 columns is illustrated in Figure 5A, which shows the total amount of SWNTs separated per column over the entire separation. According to a selective adsorption mechanism, the most strongly adsorbing SWNT chirality should out-compete the remaining species in early columns, and only after the SWNTs with the largest affinity for sephacryl binding sites are removed can subsequent species be adsorbed. This mechanism then asserts that there should be an inverse relationship between total amount of SWNTs collected and column number. However, experimentally, we note minimal site occupancy by semiconducting SWNTs at early columns, as illustrated in Figure 5A.

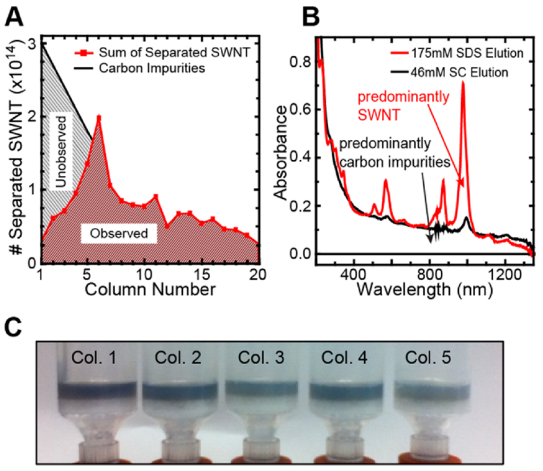

Figure 5. (A) Analysis of the total number of desorbed SWNTs measured per column over the course of 20 columns. The local maximum at column 6, followed by the further reduction of extracted SWNTs per column, suggests the presence of carbon impurities that occupy sephacryl binding sites but is not experimentally observed. A qualitative estimation for the gel occupancy of carbon impurities is denoted by the gray shaded region in columns 1−5. (B) Absorbance spectrum of the retained carbon impurities, showing the presence of mostly fullerene fragments, broken nanotubes and bundles, and a small quantity of SWNTs that is not eluted with 175 mM SDS. (C) Photograph of the first five columns after the 5 wt % SDS desorption step, showing the presence of carbon impurities that do not get removed from the column and hence occupy available binding sites on the sephacryl gel. Note the decreasing level of coloration as column number increases, indicating a reduction in the quantity of carbon impurities.

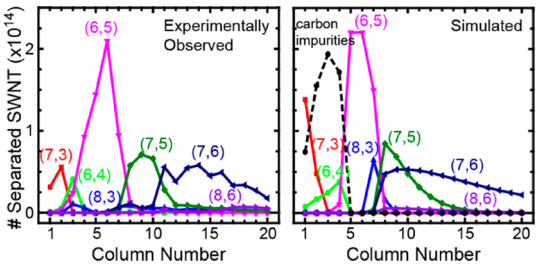

Figure 6. Chirality-specific column-by-column analysis of gel-based semiconducting SWNT separation. A direct comparison between the experimentally desorbed material over 20 columns (A) and that predicted by the model outlined here (B) qualitatively demonstrates the accuracy of a kinetically based competitive binding model to describe gel-based semiconducting SWNT separation. Specific parameters used to generate the simulation shown in (B) are listed in Table 1 as well as the text.

In this model, the addition of carbon impurities that are not eluted allows for the trend of equal or less adsorbed material per column with increasing column iterations. The amount of carbon impurities present in the starting SWNT mixture ($N_{\text{carbon impurities}}$ (col = 1, t = 0)) was allowed to vary in order to obtain the best possible agreement between experimental and modeled results.

Choosing a value for θ, which translates to the total number of binding sites per the 1.4 mL of sephacryl gel utilized per column, is not straightforward. The geometry, density, or average spacing between adjacent amide groups within this material are not known. In order to simplify this model, we approximated this complex material as a collection of equivalent binding sites that, besides their chirality-specific affinities for SWNTs, are otherwise identical. In terms of the simulation separation, we iteratively varied θ to obtain the best possible agreement between experimental and modeled results. Not surprisingly, strong agreement was achieved when θ was chosen such that it approximately matched the total amount of material eluted per column, effectively simulating the SWNT overloading conditions that have previously been reported as necessary to effectively separate SWNTs with amide-based gel.[9]

Model Validation. To simulate the SWNT separation achieved by processing the first SWNT/sephacryl column, the model uses eq 6 to calculate the number of chirality-specific binding events that occur between $N_{n,m}$ or $N_{\text{carbon impurities}}$ and θ within volume V over the course of time t. Specifically, we chose to model the experimentally utilized conditions of time t = 600 s and volume V = 0.01L (approximately equivalent to the SWNT volume, as the sephacryl volume is small) to allow for a direct comparison between the model and experiment. Following the simulation of the first SWNT/sephacryl column, quantities of $N_{n,m}$ and $N_{\text{carbon impurities}}$ were reduced by the specific amount of each that was adsorbed to the first column and then taken as the starting solution for the simulation of the second column. The second column was then simulated in an identical manner to the first, starting with θ free binding sites. Repetitions of this simulation were then used to model a separation over the experimentally relevant number of iterative columns. The basis for the experimental comparisons is summarized in a single plot which uses the aforementioned fitting procedure to extract the chirality-dependent number of separated SWNTs per column, as illustrated in Figure 6A for the 20 column separation experiment.

Using experimentally extracted values for $N_{n,m}$, $N_{\text{carbon impurities}}$, V = 0.01L, per column interaction time t = 600 s, and $\theta_T = 2.2 \times 10,^{14}$ we were able to perform a best fit analysis around each chirality-specific SWNT/sephacryl binding rate constant. The resultant model-predicted column-dependent SWNT separation is shown in Figure 6B. Best fit values for $k_{n,m}$ and $k_{\text{carbon impurities}}$ along with starting quantities for each $N_{n,m}$ and $N_{\text{carbon impurities}}$ are listed in Table 1. In the following paragraphs, we further discuss the ability of this model to describe SWNT gel-based separation and its implications on modifications of SWNT separation procedures.

A direct comparison between experimentally extracted values and modeled values of SWNTs adsorbed per column show strong agreement, as exhibited in Figure 6. The quality of this fit combined with the

relative simplicity of this model indicates that the underlying chemical process that governs this separation can be described as a kinetically driven selective adsorption of semiconducting SWNTs to sephacryl binding sites. We do not observe concentration-driven desorption of SWNTs from sephacryl when excess solvent solution is passed through the gel in the rinsing step to remove unbound SWNTs (Figure 1, step 2), hence showing no dependence of the process on a retention time as would be the case for certain types of chromatography.

Reasoning as to why the binding of semiconducting SWNTs to sephacryl at 70 mM appears irreversible, while at 175 mM release of SWNTs results in the chiral selectivity of the separation process, remains unclear. Note that while sephacryl itself is a spherically shaped cross-linked hydrogel with amide and dextran functionality,[42] this model simplifies this matrix as a series of equivalent SWNT binding sites. In reality, the binding of SWNTs to sephacryl most likely involves the interaction of a series of potentially non-equivalent amide binding sites with a single semiconducting nanotube, the sum of which constitutes the total change in free energy associated with the binding event. It is also assumed that the molar concentration of binding sites, M_θ, is fixed from column to column and here was approximated as 2.6×10^{-7} moles of sites/L, where the volume of the sephacryl is taken based on approximately 80% by volume of gel and 20% by volume of solvent (here 70 mM SDS). Further, it has been shown that the change in free energy associated with SWNT/sephacryl binding for a mixture of semiconducting SWNTs becomes more negative and thus is more favorable at SDS concentrations below 70 mM.[35]

The findings demonstrated elsewhere[34] and here further demonstrate the complex relationship between a semiconducting carbon nanotube and an immobile hydrogel with multiple functionalities, as mediated by the presence of surfactant molecules. Future studies focused on this interaction and, specifically, its reversibility as a function of SDS concentration (desorption not modeled here) need to be conducted in order to better understand and more fully control the gel-based SWNT separation process.

Single-Chirality SWNT Separation Scale Up. Here, we have laid the foundations for the classification of sephacryl-gel-mediated SWNT separation as a kinetically driven selective adsorption process. Hence, this system behaves more similarly to an adsorption chromatography, where the eluent is different from the first solvent. As such, one does not expect this methodology to suffer from the scaling issues associated with retention time-dependent chromatography-based separations. To test this, we first utilized our model to simulate the expected outcome of a separation carried out under both native (described earlier) and 15 times scaled up conditions. Specifically, scaled conditions were simulated such that amount of starting material of semiconducting

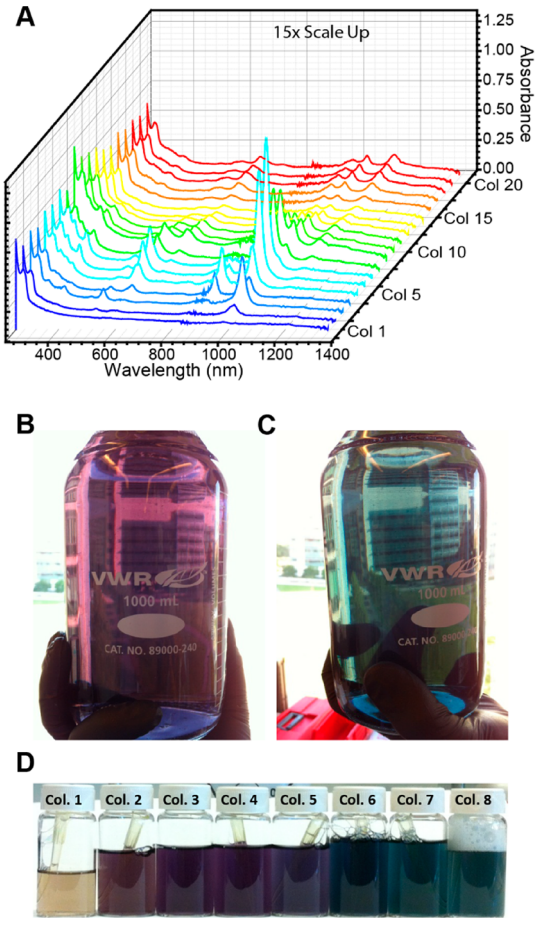

Figure 7. Demonstrations of the advantages of SWNT separation *via* a scalable process. (A) Absorbance spectra of the SWNT separated as a 15× scale up. (B,C) Large volumes of single-chirality semiconducting (6,5) (B) and semiconduting mixed chirality (7,5), (7,6), and (8,3) (C) can be generated using fewer procedural iterations. (D) By intentionally choosing to not fully scale the 175 mM SDS volume used during the desorption step, it is possible to desorb SWNTs into smaller liquid volumes, resulting in the separation of more concentrated solutions—col 4 shows an optical density of 4.8 with a 1 cm path length. Note that to capture images B and C it was necessary to place the vessels in front of an open window on a sunny day due to the path length and optical density of the samples.

SWNTs, carbon impurities, and sephacryl binding sites, along with reactor volume and total interaction time, were all 15 times that of the native conditions, and all other reaction assumptions and modeling procedures remained constant. The experimentally realized separation for a 15 times scale up, which showed nearly identical per column chirality contents as the native separation, is shown in Figure 7A.

To take advantage of the predicted scalability of this process, we carried out a 20 column separation at 15 times scale and found that, indeed, the resultant per column extracted semiconducting SWNT was qualitatively similar to that obtained from a native scale separation. The successful scaling of this separation process allowed for two distinct advantages regarding SWNT separation that are not possible at native scaling.

First, scaling of the SWNT separation process allows for the collection of large volumes of single-chirality semiconducting SWNT material through fewer procedural iterations. Through scaling, it was possible for us to accumulate liters of both single-chirality and selective-chirality semiconducting samples over a relatively short period of time. Here, we show liter quantities of both single-chirality (6,5) and mixed-chirality (7,5), (7,6), and (8,3) in Figure 7B,C, respectively. The ability to quickly generate large quantities of separated single-chirality SWNTs has advantages on the laboratory scale, where construction of macroscopic films or other SWNT solids from pure materials necessarily requires quantities of SWNTs that would be significantly more laborious to produce using separation based on density gradient ultracentrifugation. Also, generation of large quantities of material bolsters the feasibility of single-chirality semiconducting SWNTs as an industrial-scale material, making possible further investigations into the unique properties of single-chirality SWNTs and how those properties can be utilized within next generation electronic and optical devices.

Second, scaling of the SWNT separation process allows for the generation of high-density single-chirality semiconducting SWNT solutions. In order to concentrate the SWNT desorbed from the sephacryl during processing of a scaled separation, we intentionally decreased the volume of 175 mM SDS used during that step. By reducing the 175 mM SDS volume 4 times, we found that it was possible to selectively desorb SWNTs into a smaller volume, resulting in a more concentrated solution (Figure 7D). It is important to note, however, that a small portion of the desorbed SWNTs is not collected by the smaller 175 mM SDS volume, most likely due to the incomplete desorption caused by reduced total interaction time between adsorbed SWNTs and the desorption solution. Despite this small loss, however, a 4 times reduction in 175 mM SDS volume allowed for us to attain 20 mL of single-chirality (6,5) samples with optical densities of approximately 4.8 using a 1 cm path length (Figure 7D, column 4). The straightforward generation of high-density single-chirality semiconducting SWNT samples is advantageous when using these materials as biosensors, as sensor signal scales proportionally with total sensor concentration.

CONCLUSION

This study has demonstrated the ability to predictably reproduce and scale a gel-based separation of SWNTs that allows one to obtain pure single-chirality samples in large quantities in a single-pass separation process. We were able to make this advancement by achieving thorough understanding of the SWNT separation mechanism as a competitive kinetic adsorption. By creating a model, we could accurately reproduce the dynamic binding and elution of each chirality, allowing us to estimate chiral-specific rate constants. This simple, descriptive model for SWNT separation describes the process level physics of this system, and the rate constants were determined based on the outcome of this separation. However, the fundamental question of what leads to the difference in rate constants among various chiralities of SWNTs and why SDS-wrapped SWNTs allow for single-chirality separation remain speculative.[9,34] Further studies are necessary to understand this complex system, and with such an understanding, we expect the costs associated with single-chirality SWNT separation to reduce dramatically. Recent work by Park *et. al.* demonstrates the commercial potential for SWNTs as transistors.[43] Once large-scale, inexpensive production of single-chirality SWNTs is a reality, such advancement stands to substantially influence both the fields of optoelectronics and biological sensing.

METHODS

Preparation of Aqueous SWNT Suspension. Raw HiPco SWNT (Unidym, lot R0513) was first processed using the organic aqueous phase separation suggested by the manufacturer for the creation of solid SWNT samples. Specifically, deionized water was added to solid SWNT cake at 20 mL/g, vigorously stirred, and transferred to a separation funnel. A small aliquot of hexane was then added, and the mixture was stirred and allowed to form a phase separation. Iterations of hexane addition, stirring, and separation were repeated until no black SWNT flakes appeared in the aqueous phase, which was yellow in color and contained non-SWNT materials remaining from the HiPco synthesis process. The aqueous phase was removed from the funnel *via* phase-separated gravity extraction. The organic phase, which contained the purified SWNTs, was transferred to a storage container and placed in a drying oven at ~120 °C until completely dry, typically 24−48 h. Finally, the resultant SWNT powder was homogenized *via* grinding with a mortar and pestle.

A SWNT suspension at 1 mg/mL in sodium dodecyl sulfate (SDS, Sigma) was generated by weighing out 100 mg of SWNT into a 250 mL beaker and adding 100 mL of an aqueous solution of 70 mM SDS. This solution was subjected to mild bath sonication (Branson 2510) for 5 min to break apart macroscopic SWNT pieces. The beaker containing the homogenized SWNT solution was placed into a temperature-controlled bath held at ~4−5 °C and subjected to tip sonication at 20 W for 20 h (Branson Digital Sonifier 250, Cole Parmer 04710−40 1/2″ tip, tip placed ~10 mm from bottom of beaker). We have found that, in order to ensure repeatability during the sonication procedure, it is possible to use relative RBM Raman peak heights. A full study of the effect of sonication and its correlation with RBM characteristics will be published elsewhere. Immediately following tip sonication, the sample was subjected to ultracentrifugation at 187 000*g* for 4 h (32 000 rpm, Beckman Coulter Optima L100 XP, SW 32 Ti Rotor, Beckman 344058 40 mL tubes). The top 90% of the supernatant was then removed from each ultracentrifuge tube and used immediately as the initial sample for the primary-pass single-chirality semiconducting SWNT separation procedure described below. Typical absorbance and Raman spectra of an initial SWNT sample are provided in Figure S1.

Primary-Pass Single-Chirality Semiconducting SWNT Separation. Ten milliliters of the prepared SWNT suspension was passed through a 1.4 mL stationary bed of 70 mM SDS equilibrated

Sephacryl S200 gel, which was held in place by the porous frit of a Pierce Biosciences 10 mL column (product #29924) (Figure 1, step 1). Flow rate of SWNTs through the gel medium was held at 1 mL/min, controlled by sealing the top of each column with a needle-pierced rubber stopper, and using a syringe pump to control column overpressure.

After passing the entirety of the SWNT solution, the sephacryl gel was then washed with 4 mL of 70 mM SDS solution under atmospheric conditions (*i.e.*, flow rate was not controlled), which removed residual SWNT solution from the gel, but retained physically adsorbed materials (Figure 1, step 2). Following the rinsing step, the column was eluted with 4 mL of neat 175 mM SDS solution under atmospheric conditions, which removed previously adsorbed material from the sephacryl gel and allowed for its collection as a separated SWNT sample (Figure 1, step 3). This process was iterated using the flow through from step 1 as the starting material for the subsequent iteration.

Conflict of Interest: The authors declare no competing financial interest.

Acknowledgment. This work was financially supported by the U.S. Department of Energy (Grant No. ER46488). R.M.J. gratefully acknowledges support from the National Science Foundation Graduate Research Fellowship and the Department of Defense through the National Defense Science and Engineering Graduate Fellowship. This work was also supported in part (author A.J.H.) by the Department of Energy Office of Science Graduate Fellowship Program (DOE SCGF), made possible in part by the American Recovery and Reinvestment Act of 2009, administered by ORISE-ORAU under Contract No. DE-AC05-06OR23100. The authors would also like to thank Zachary W. Ulissi for helpful discussions.

Supporting Information Available: Initial SWNT sample preparation along with Raman and absorption spectroscopy analysis; waterfall absorption plot of separated SWNTs; discussion and analysis of SWNT absorption profile fitting procedure; discussion and analysis of the equivalency of separation achieved by flowing through and stirring methodologies; and details for calculating the simulated separation. This material is available free of charge *via* the Internet at http://pubs.acs.org.

REFERENCES AND NOTES

1. Liu, Z.; Tabakman, S.; Welsher, K.; Dai, H. Carbon Nanotubes in Biology and Medicine: *In Vitro* and *In Vivo* Detection, Imaging and Drug Delivery. *Nano Res.* **2009**, *2*, 85–120.
2. Boghossian, A. A.; Zhang, J.; Barone, P. W.; Reuel, N. F.; Kim, J.-H.; Heller, D. A.; Ahn, J.-H.; Hilmer, A. J.; Rwei, A.; Arkalgud, J. R.; *et al.* Near-Infrared Fluorescent Sensors Based on Single-Walled Carbon Nanotubes for Life Sciences Applications. *ChemSusChem* **2011**, *4*, 848–863.
3. Avouris, P.; Freitag, M.; Perebeinos, V. Carbon-Nanotube Photonics and Optoelectronics. *Nat. Photonics* **2008**, *2*, 341–350.
4. LeMieux, M. C.; Sok, S.; Roberts, M. E.; Opatkiewicz, J. P.; Liu, D.; Barman, S. N.; Patil, N.; Mitra, S.; Bao, Z. Solution Assembly of Organized Carbon Nanotube Networks for Thin-Film Transistors. *ACS Nano* **2009**, *3*, 4089–4097.
5. Opatkiewicz, J.; LeMieux, M. C.; Bao, Z. N. Nanotubes on Display: How Carbon Nanotubes Can Be Integrated into Electronic Displays. *ACS Nano* **2010**, *4*, 2975–2978.
6. Bindl, D. J.; Brewer, A. S.; Arnold, M. S. Semiconducting Carbon Nanotube/Fullerene Blended Heterojunctions for Photovoltaic Near-Infrared Photon Harvesting. *Nano Res.* **2011**, *4*, 1174–1179.
7. Reich, S.; Thomsen, C.; Maultzsch, J. *Carbon Nanotubes—Basic Concepts and Physical Properties*, 1st ed.; Wiley-VCH: Weinheim, Germany, 2004.
8. Moshammer, K.; Hennrich, F.; Kappes, M. M. Selective Suspension in Aqueous Sodium Dodecyl Sulfate According to Electronic Structure Type Allows Simple Separation of Metallic from Semiconducting Single-Walled Carbon Nanotubes. *Nano Res.* **2009**, *2*, 599–606.
9. Liu, H. P.; Nishide, D.; Tanaka, T.; Kataura, H. Large-Scale Single-Chirality Separation of Single-Wall Carbon Nanotubes by Simple Gel Chromatography. *Nat. Commun.* **2011**, 2.
10. Li, X.; Tu, X.; Zaric, S.; Welsher, K.; Seo, W. S.; Zhao, W.; Dai, H. Selective Synthesis Combined with Chemical Separation of Single-Walled Carbon Nanotubes for Chirality Selection. *J. Am. Chem. Soc.* **2007**, *129*, 15770–15771.
11. Li, Y. M.; Mann, D.; Rolandi, M.; Kim, W.; Ural, A.; Hung, S.; Javey, A.; Cao, J.; Wang, D. W.; Yenilmez, E.; *et al.* Preferential Growth of Semiconducting Single-Walled Carbon Nanotubes by a Plasma Enhanced CVD Method. *Nano Lett.* **2004**, *4*, 317–321.
12. South West NanoTechnologies; http://swentnano.com (accessed December 14, 2012).
13. Krupke, R.; Hennrich, F.; Kappes, M. M.; Lohneysen, H. V. Surface Conductance Induced Dielectrophoresis of Semiconducting Single-Walled Carbon Nanotubes. *Nano Lett.* **2004**, *4*, 1395–1399.
14. Krupke, R.; Hennrich, F.; von Lohneysen, H.; Kappes, M. M. Separation of Metallic from Semiconducting Single-Walled Carbon Nanotubes. *Science* **2003**, *301*, 344–347.
15. Vetcher, A. A.; Srinivasan, S.; Vetcher, I. A.; Abramov, S. M.; Kozlov, M.; Baughman, R. H.; Levene, S. D. Fractionation of SWNT/Nucleic Acid Complexes by Agarose Gel Electrophoresis. *Nanotechnology* **2006**, *17*, 4263–4269.
16. Lustig, S. R.; Jagota, A.; Khripin, C.; Zheng, M. Theory of Structure-Based Carbon Nanotube Separations by Ion-Exchange Chromatography of DNA/CNT Hybrids. *J. Phys. Chem. B* **2005**, *109*, 2559–2566.
17. Tu, X. M.; Manohar, S.; Jagota, A.; Zheng, M. DNA Sequence Motifs for Structure-Specific Recognition and Separation of Carbon Nanotubes. *Nature* **2009**, *460*, 250–253.
18. Zheng, M.; Jagota, A.; Strano, M. S.; Santos, A. P.; Barone, P.; Chou, S. G.; Diner, B. A.; Dresselhaus, M. S.; McLean, R. S.; Onoa, G. B.; *et al.* Structure-Based Carbon Nanotube Sorting by Sequence-Dependent DNA Assembly. *Science* **2003**, *302*, 1545–1548.
19. Zheng, M.; Jagota, A.; Semke, E. D.; Diner, B. A.; McLean, R. S.; Lustig, S. R.; Richardson, R. E.; Tassi, N. G. DNA-Assisted Dispersion and Separation of Carbon Nanotubes. *Nat. Mater.* **2003**, *2*, 338–342.
20. Strano, M. S.; Zheng, M.; Jagota, A.; Onoa, G. B.; Heller, D. A.; Barone, P. W.; Usrey, M. L. Understanding the Nature of the DNA-Assisted Separation of Single-Walled Carbon Nanotubes Using Fluorescence and Raman Spectroscopy. *Nano Lett.* **2004**, *4*, 543–550.
21. Kim, W. J.; Usrey, M. L.; Strano, M. S. Selective Functionalization and Free Solution Electrophoresis of Single-Walled Carbon Nanotubes: Separate Enrichment of Metallic and Semiconducting SWNT. *Chem. Mater.* **2007**, *19*, 1571–1576.
22. Strano, M. S.; Dyke, C. A.; Usrey, M. L.; Barone, P. W.; Allen, M. J.; Shan, H. W.; Kittrell, C.; Hauge, R. H.; Tour, J. M.; Smalley, R. E. Electronic Structure Control of Single-Walled Carbon Nanotube Functionalization. *Science* **2003**, *301*, 1519–1522.
23. Rauwald, U.; Shaver, J.; Klosterman, D. A.; Chen, Z. Y.; Silvera-Batista, C.; Schmidt, H. K.; Hauge, R. H.; Smalley, R. E.; Ziegler, K. J. Electron-Induced Cutting of Single-Walled Carbon Nanotubes. *Carbon* **2009**, *47*, 178–185.
24. Arnold, M. S.; Green, A. A.; Hulvat, J. F.; Stupp, S. I.; Hersam, M. C. Sorting Carbon Nanotubes by Electronic Structure Using Density Differentiation. *Nat. Nanotechnol.* **2006**, *1*, 60–65.
25. Ghosh, S.; Bachilo, S. M.; Weisman, R. B. Advanced Sorting of Single-Walled Carbon Nanotubes by Nonlinear Density-Gradient Ultracentrifugation. *Nat. Nanotechnol.* **2010**, *5*, 443–450.
26. Green, A. A.; Hersam, M. C. Nearly Single-Chirality Single-Walled Carbon Nanotubes Produced *via* Orthogonal Iterative Density Gradient Ultracentrifugation. *Adv. Mater.* **2011**, *23*, 2185–2190.
27. Antaris, A. L.; Seo, J. W. T.; Green, A. A.; Hersam, M. C. Sorting Single-Walled Carbon Nanotubes by Electronic Type Using Nonionic, Biocompatible Block Copolymers. *ACS Nano* **2010**, *4*, 4725–4732.
28. Arnold, M. S.; Stupp, S. I.; Hersam, M. C. Enrichment of Single-Walled Carbon Nanotubes by Diameter in Density Gradients. *Nano Lett.* **2005**, *5*, 713–718.

29. Green, A. A.; Duch, M. C.; Hersam, M. C. Isolation of Single-Walled Carbon Nanotube Enantiomers by Density Differentiation. *Nano Res.* **2009**, *2*, 69–77.
30. Tanaka, T.; Liu, H.; Fujii, S.; Kataura, H. From Metal/Semiconductor Separation to Single-Chirality Separation of Single-Wall Carbon Nanotubes Using Gel. *Phys. Status Solidi (RRL)* **2011**, *5*, 301–306.
31. NanoIntegris; http://www.nanointegris.com (accessed December 14, 2012).
32. Jain, R. M.; Howden, R.; Tvrdy, K.; Shimizu, S.; Hilmer, A. J.; McNicholas, T. P.; Gleason, K. K.; Strano, M. S. Polymer-Free Near-Infrared Photovoltaics with Single Chirality (6,5) Semiconducting Carbon Nanotube Active Layers. *Adv. Mater.* **2012**, *24*, 4436–4439.
33. Nair, N.; Kim, W. J.; Braatz, R. D.; Strano, M. S. Dynamics of Surfactant-Suspended Single-Walled Carbon Nanotubes in a Centrifugal Field. *Langmuir* **2008**, *24*, 1790–1795.
34. Silvera-Batista, C. A.; Scott, D. C.; McLeod, S. M.; Ziegler, K. J. A Mechanistic Study of the Selective Retention of SDS-Suspended Single-Wall Carbon Nanotubes on Agarose Gels. *J. Phys. Chem. C* **2011**, *115*, 9361–9369.
35. Hirano, A.; Tanaka, T.; Kataura, H. Thermodynamic Determination of the Metal/Semiconductor Separation of Carbon Nanotubes Using Hydrogels. *ACS Nano* **2012**, *6*, 10195–10205.
36. Schoppler, F.; Mann, C.; Hain, T. C.; Neubauer, F. M.; Privitera, G.; Bonaccorso, F.; Chu, D. P.; Ferrari, A. C.; Hertel, T. Molar Extinction Coefficient of Single-Wall Carbon Nanotubes. *J. Phys. Chem. C* **2011**, *115*, 14682–14686.
37. Ju, S. Y.; Utz, M.; Papadimitrakopoulos, F. Enrichment Mechanism of Semiconducting Single-Walled Carbon Nanotubes by Surfactant Amines. *J. Am. Chem. Soc.* **2009**, *131*, 6775–6784.
38. LeMieux, M. C.; Roberts, M.; Barman, S.; Jin, Y. W.; Kim, J. M.; Bao, Z. N. Self-Sorted, Aligned Nanotube Networks for Thin-Film Transistors. *Science* **2008**, *321*, 101–104.
39. Hirano, A.; Tanaka, T.; Kataura, H. Adsorbability of Single-Wall Carbon Nanotubes onto Agarose Gels Affects the Quality of the Metal/Semiconductor Separation. *J. Phys. Chem. C* **2011**, *115*, 21723–21729.
40. Nair, N.; Usrey, M. L.; Kim, W. J.; Braatz, R. D.; Strano, M. S. Estimation of the (*n*,*m*) Concentration Distribution of Single-Walled Carbon Nanotubes from Photoabsorption Spectra. *Anal. Chem.* **2006**, *78*, 7689–7696.
41. Naumov, A. V.; Ghosh, S.; Tsyboulski, D. A.; Bachilo, S. M.; Weisman, R. B. Analyzing Absorption Backgrounds in Single-Walled Carbon Nanotube Spectra. *ACS Nano* **2011**, *5*, 1639–1648.
42. GE Lifesciences; http://www.gelifesciences.com/webapp/wcs/stores/servlet/catalog/en/GELifeSciences/brands/sephacryl/ (accessed December 14, 2012).
43. Park, H.; Afzali, A.; Han, S.-J.; Tulevski, G. S.; Franklin, A. D.; Tersoff, J.; Hannon, J. B.; Haensch, W. High-Density Integration of Carbon Nanotubes *via* Chemical Self-Assembly. *Nat. Nanotechnol.* **2012**, *7*, 787–791.